



LARGE WAVES IN THICK INTERIOR SAKHALIN PACK ICE

J.R. Marko

ASL Environmental Sciences Inc., Sidney, B.C., Canada

ABSTRACT

Results are reported describing anomalously strong waves-in-ice signals detected by a large array of bottom-moored upward-looking IPS-4 ice profilers deployed in continental shelf waters east of Sakhalin Island adjacent to Acoustic Doppler Current Profiler (ADCP) instrumentation capable of measuring ice drift velocities. Data recovered from several years of such deployments allowed identification of numerous segments of ice draft time series data containing signatures distinctive of ocean gravity waves in the interior of the seasonally southward drifting regional ice pack. Data are presented here from a time interval coincident with the passage of an intense cyclone as acquired at 8 widely-spaced monitoring stations, all initially more than 300 km from open water wave source areas. Results obtained in 9-10/10 concentrations of ice with mean drafts ranging between 1 and 2 m, showed surprisingly large concentrations of wave energy in the central portion of the monitoring array at separations no closer than about 150 km from the 5/10 ice boundary. The progress of the observed disturbances was quantified in time and space in terms of propagation speeds and directions and associated attenuation coefficients. The large deduced wave amplitudes (peak rms values $> 1\text{m}$) and low propagation speeds (1-2m/s) are not readily explained by conventional flexural wave- or wave-scattering theories. Interpretations of the results are presented based upon modifications of the ice pack's wave propagation properties by wind-forcing.

INTRODUCTION

Most observations of ocean gravity waves in heavy sea ice either take place in outer portions of marginal ice zones or involve very long period (20-30 sec) swell characterized by attenuation rates low enough to allow detection hundreds of kilometres inside Polar ice packs. Data are presented here on much shorter period waves observed with amplitudes as large as 1 m or more in thick pack ice at distances on the order of 300 km from the nearest open water wave sources. Detection of such waves utilized upward-looking sonar (ULS) instruments deployed as part of a three-year environmental study program carried out in preparation for hydrocarbon production in the Sea of Okhotsk by Exxon and Sakhalin Energy. The presented results will be confined to description and initial interpretations of a single waves-in-ice event which occurred during an approximately two-day March, 1998 interval associated with the passage of a strong cyclone. Focus will be given to describing this event and to identifying the circumstances which gave rise to its occurrence and which could, presumably, produce similar phenomena elsewhere. Tentative results from more quantitative comparisons with possible generation and propagation mechanisms will also be presented.

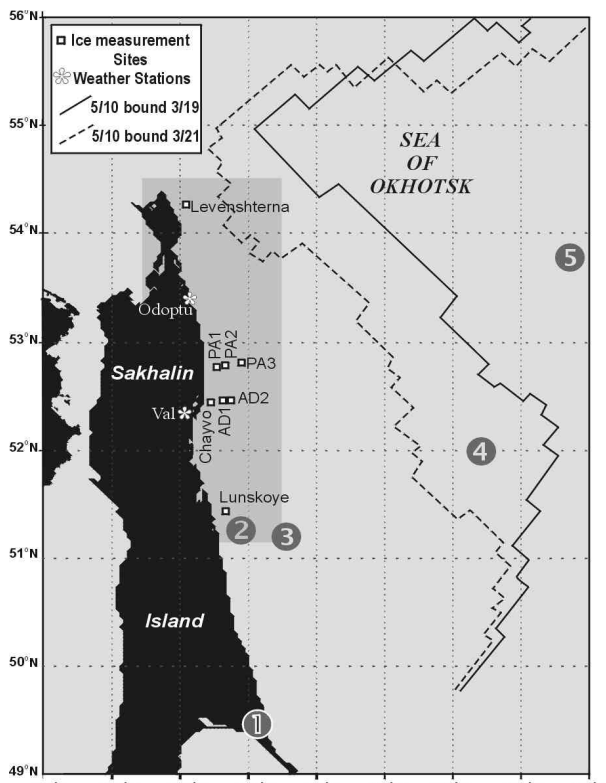


Figure 1. JIP ice monitoring and meteorological sites in the Sea of Okhotsk. March 19 and March 21 5/10 ice concentration boundaries and the approximate positions of the cyclone minima are shown successively numbered at 6-hour intervals from 1800, March 20, 1998.

Mooring separations at a given monitoring site were short enough (< 100 m) to assure collection of data representative of a common location. Ranges were converted into corresponding draft values using hydrostatic pressures recorded on-board each IPS4 instrument together with regional surface air pressure data and estimates of sound speed updated by ranges to the sea surface established from measurements on patches of open water/thin ice. On-board water temperature and instrument tilt data, as well as CTD profiles obtained during instrument deployments, were also utilized in the conversion process. The resulting draft time series were further translated into draft versus distance representations of ice bottom topography using ice velocities derived from ADCP or WHISL data sets. Given the 20 cm/s ice drift velocities typical of the study area, ice draft data were typically obtained, with accuracies better than 20 cm, at 50 cm intervals along the ice undersurface passing over each site.

METHODOLOGY AND ENVIRONMENTAL CONDITIONS

Sub-Surface Measurement Program

The 1997-1998 JIP (Joint Industry Program) environmental studies in the Sea of Okhotsk provided measurements of ice-draft, -drift velocity and current profiles on the continental shelf east of Sakhalin Island (Figure 1) at eight regional sites in water depths between 70-74 m (Levenshterna, and PA3) and 26.5 m (Chayvo). Separate moorings at each site contained:

- a) an ASL Environmental Sciences IPS-4 Ice Profiling Sonar which sampled ice undersurface ranges @ 1 Hz with a narrow 2°, 400 kHz acoustic beam ; and
- b) either: 1) an RDI Workhorse 300Khz ADCP (Acoustic Doppler Current Profiler) with “bottom-tracking” capability or; 2) a WHISL (Woods Hole Instrument Systems model SP2000) electromagnetic current meter.

Meteorological and Ice Conditions

The intense waves-in-ice activity coincided with the N-NE-directed passage of the cyclone over the March 19-21 period. Positions of the disturbances pressure minimum, taken from Japan Meteorological Agency charts, are denoted in Figure 1 at 6-hour intervals over the period 0600, March 20 through 0600, March 21 (all times are referenced to Universal Coordinated Time (UTC)). It is seen that the depression moved from an initial position south of the study area to roughly 50 km E-SE of the southernmost, Lunskoye, monitoring site by 1800, March 20 when the pressure minimum dipped as low as 964 mb before rising with further E-NE movement. Accompanying changes in surface pressure, wind direction and wind speed are evident in Val coastal station (52° 20' N, 143° 05' E) data (Figure 2).

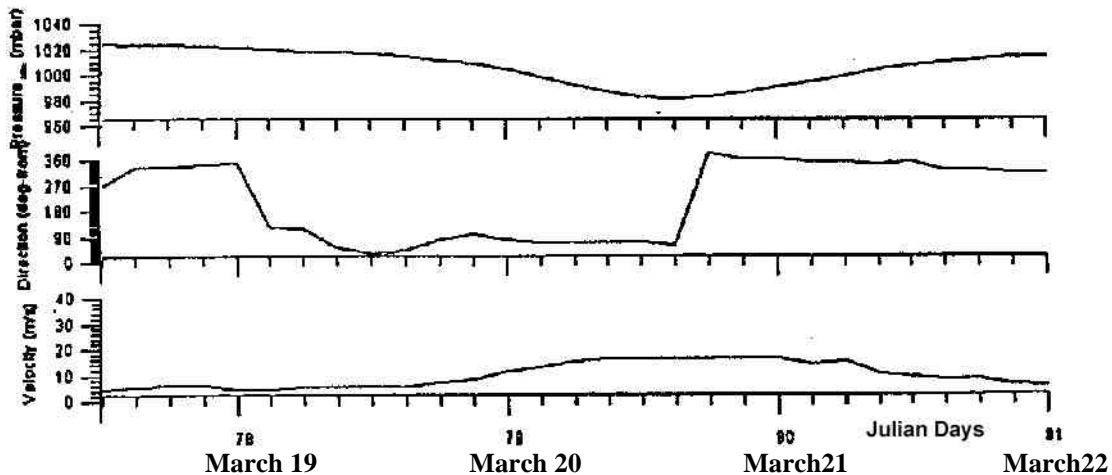


Figure 2. Meteorological data recorded at Val

Although cloud coverage precluded useful satellite observations during the waves-in-ice event, a March 19 NOAA AVHRR image showed the extreme northern and southern sites under heavy, 9/10-10/10, ice as well as slightly lower ice concentrations at the central sites, primarily in the form of individual floes with linear dimensions ranging up to 10 or 15 km. The westernmost central sites, PA1 and Chayvo, were under ice at the eastern edge of a large

coastal polynya. Subsequent dramatic changes in the regional pack over the next 2 days were indicated by ice concentration contours derived from 25 km spatial resolution SSM/I passive microwave data acquired by a Defence Meteorological Satellite Program (DMSP) satellite on March 19 and 21. As indicated by the contours plotted in Figure 1, these data were consistent with occurrence of a massive, approximately 80 km, westward shift of the 5/10 ice boundary east of the central sites over the intervening period, presumably under the March 20 easterly wind forcing (Figure 2). Nevertheless, even on March 21, ice at concentrations lower than 5/10 apparently came no closer than 155 km to the nearest central monitoring site (PA3). With the 1.6/10 (16 %) ice concentration boundary lying a further 185 km offshore, the PA3 site was more than 300 km from open water in the eastern Sea of Okhotsk throughout the waves-in-ice event. U.S. National Ice Center chart data suggesting the presence of ice with thicknesses 30-70 cm and 70-120 cm in the study area prior to March 20 were compatible with ice drafts derived from IPS-4 data recorded throughout the event. Specifically, hourly-averaged data for the period 1600, March 20 to 0000, March 22 showed drafts increasing in both the east to west and south to north directions. Few hourly values were less than 1 m and drafts in excess of 2m were common at the PA1 and Chayvo sites. Still larger average draft values were encountered, at times, at the northernmost, Levenshterna, site. At all sites, concentrations rarely descended below the 9/10 (90%) coverage level and then only at the most offshore and southern central sites, AD1 and AD2 and at Lunskeye. Progressive displacement plots for ice at the six ADCP-equipped monitoring sites for the period 1200, March 19 to 0000, March 22 showed the inferred rapid westward ice movements at the central sites (see the representative PA3 results in Figure 3) began at, roughly, 0000, March 20 (Julian Day 79.0) and persisted until about 1800, March 20, corresponding to an overall average westward speed component of 40 cm/s (0.8 kt). Much smaller westward drifts were recorded at the peripheral Levenshterna and Lunskeye sites (Figure 3). It is significant to note that, except near Chayvo where the initial width of the polynya was exceptionally large, net westerly drifts at the central sites were several times smaller than the average 80 km shift associated with the 5/10 concentration boundary over the same period (Figure 1). This circumstance is consistent with westward increasing resistance to westward drift arising from the closing of the coastal polynya and ice pileup and compaction. It is also significant that southward ice drift at the central sites only reappeared at, roughly, 1200, March 20, coinciding with the easterly to northerly wind shift which accompanied the eastward shift of the cyclone away from the Sakhalin coastline.

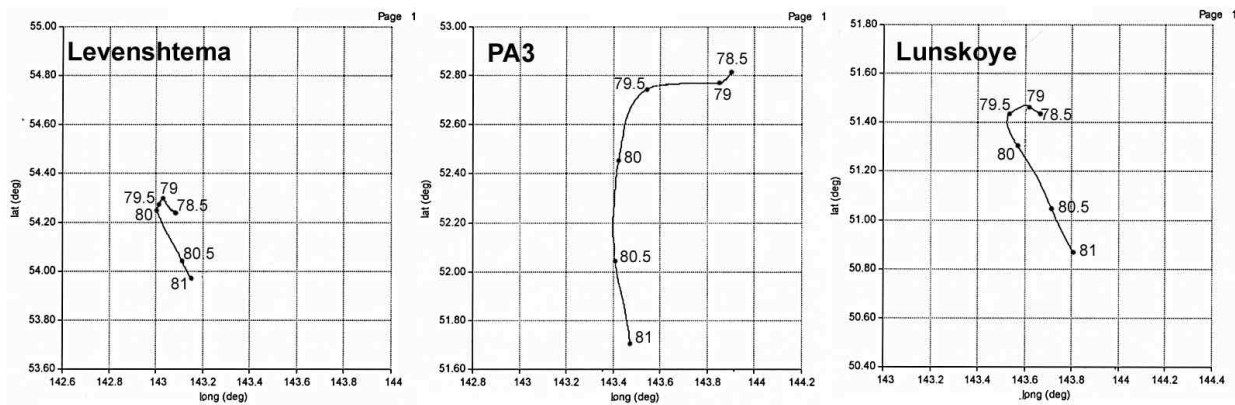


Figure 3. Progressive displacement plots for ice movements at all ADCP-equipped sites for the period 1200, March 19 (day 78.5 to 0000, March 22 (Day 81).

WAVES-IN-ICE AND CURRENT DATA

With the outermost, PA3, site at least 150 km west of the 5/10 concentration boundary and 9-10/10 concentrations of 1.5-2.5 m thick ice present at all central sites, initial evidence of large amplitude, periodic wave-like components in the draft data recorded at such sites was viewed with some skepticism. The apparent absence of similar activity at the northern Levenshterna site, which was only about 35 km inshore of the 5/10 ice boundary and equally exposed to waves from potential eastern wave source areas, also encouraged interpretive caution. Nevertheless, time series results (Figure 4a) showed the unambiguous periodic and negative-going draft variations expected from wave-driven vertical oscillations of the ice undersurface. Moreover, these oscillations had similar counterparts in the IPS-4 hydrostatic pressure data records.

Spectral analyses (Figure 4b) of data recorded at times close to estimated peak wave intensity at site PA3 showed the wave activity to be narrowband and centred at approximately 0.072 Hz (14 second wave period). Spectra computed for the shallower PA2 and PA1 sites showed clear evidence of progressive attenuation of wave energy with increasing separation from presumed eastern wave source areas and shoreward narrowing of the spectral peak. The latter effect was consistent with the suppression of higher frequency wave components by the tendency of the ice medium to act as a low-pass filter on incident gravity waves.

The narrow spectral range of the observed phenomena facilitated separation of wave- and ice-topography-related components of the draft time series data. Temporal and spatial variations in the wave-related components were quantified through successive applications of digital band-pass and low-pass filters chosen for sensitivity to wave energy variability on time scales longer than, roughly, 1 hour. Detailed intensity (defined as the squared amplitude of the filtered draft data) versus time results are plotted in Figure 5 for all sites during the period 0000, March 19 to 1600, March 23. The information presented for each site includes representations of total near-surface current (tidal + residual) for the shorter period 0600, March 20 through 0000, March 22 associated with all but the latest stages of the waves-in-ice events. The vectors plotted for each of six ADCP-equipped sites represent currents at 6-8 m depths as averaged over each of the six hourly 3-minute measurement intervals. The barotropic nature of the flow indicated by the full body of profile results allows reasonable comparisons of these data with the hourly-averaged near-bottom currents plotted for the WHISL-equipped PA2 and AD1 sites.

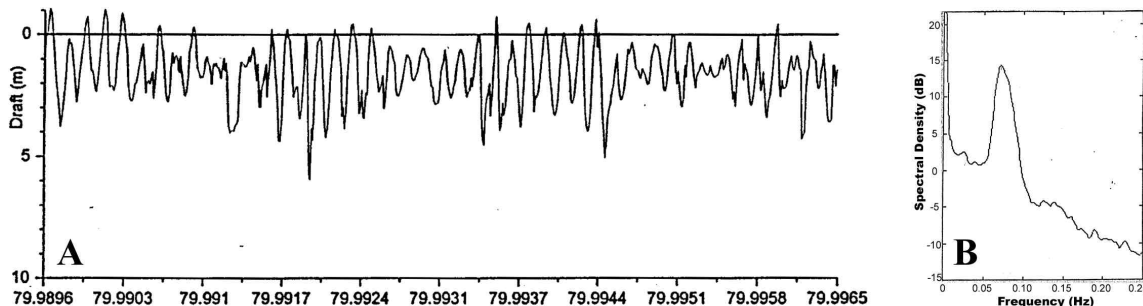


Figure 4. A) Ice draft times series for the site PA3 during a 10-minute period centred on Julian Day 79.9931 (2350, March 20, 1998); and B) temporal spectrum for IPS-4 data recorded at the same site during the period 0144-0531, March 21.

The wave intensity plots (Figure 5) show the first evidence of a waves-in-ice event appeared at the Lunskeye and PA3 sites at about 1800, March 20. The latest first appearance of wave disturbance occurred at the Levenshterna site, although the wave signals detected at this location and at the other “non-central” site, Lunskeye, were only marginally above background. Intensities were progressively decreased in magnitude and delayed in arrival with shoreward displacement. No universal “shape” or time dependence was observed in the individual site wave intensities. Differences in this respect were particularly evident between inshore (PA1 and Chayvo) and offshore (PA3, PA2, AD2, AD1) sites. Specifically, inshore site intensity fluctuations showed: characteristically larger amplitudes; lower temporal frequencies; and longer durations of wave activity relative to observations at more offshore sites.

The current data in Figure 5 show strong southward flows to have been initiated shortly before 1800, March 20 at the more southern and inshore sites (Lunskeye, Chayvo and PA1), with maximal near-surface flows increasing in a north to south direction and peaking at speeds between 60 and 100 cm/s. This southward current buildup was, roughly, coincident with the above-noted switch to northerly winds and the appearance of strong southerly ice drift components. As in the ice drift results, current changes were greatly diminished and delayed by about 16 hours at the northern, Levenshterna, site.

Reviews of the combined data sets suggest that a local sustained southward current presence was a necessary but not sufficient condition for detectable wave activity at a given site. Likewise, sites associated with such activity at times within 1 or 2 hours of local southward current development were either those closest to the 5/10 ice concentration boundary (Levenshterna and PA3) or were inshore of ice largely excluded from the preceding interval of westward ice drift (Lunskeye). As well, it is notable that peripheral site (Levenshterna and Lunskeye) wave intensities exhibited no obvious dependences upon southward current strength unlike central site intensities which peaked well after initiation of southward flow and within a few hours of maximal current speeds.

DATA ANALYSES AND INTERPRETATION

Use of the data of Figure 5 to quantitatively describe and understand the origins of the observed waves-in-ice event was complicated by the noted site-to-site differences in temporal intensity variability which precluded use of simple cross-correlation techniques for estimating speeds and directions associated with propagation of the underlying wave phenomena. Consequently, propagation data were obtained assuming one to one correspondences among first signal arrivals at all individual sites. Timings of such arrivals were established by ignoring time series data corresponding to intensities smaller than roughly 0.015 m^2 which preceded the sharp initial rises in intensity observed at all central sites (Figure 5). This restriction did not allow detailed timing estimates for the 2 peripheral sites characterized by marginal intensities. Elsewhere, the arrival times, defined by intersections of the time axis with straight-line projections of the initial sharp intensity rises, allowed calculation of “effective delays” over paths separating pairs of monitoring sites. Corresponding attenuation rates were calculated from the ratios of amplitudes of peak intensities as computed for the sites at the ends of each path. RMS values of these peak amplitudes, A_{peak} , ranged between 0.59 m (Chayvo) and 1.08 m (PA3), with the latter value, observed in ice of 1.5 m average thickness, equivalent to a 4.32 m significant peak to peak wave height. Computation of

propagation parameters was carried out using groups of 3 sites among which timing and amplitude differences could be calculated corresponding to 2 separate, non-parallel, paths, each linking a different site to a designated, common “vertex” site. Three such groups are listed in Table 1, each spanning a slightly different portion of the monitoring region. The vertex site in each group is readily identified as the first site specified in the nomenclature used to designate each of the group’s two member pairs. Within each group, propagation parameters derived for each of the two constituent paths allow unambiguous estimation of parameters describing common parallel wavefronts propagating through all three member sites. The group associated with the constituent paths PA3-PA2 and PA3-AD1 provides data representative of waves in the outer portion of the monitoring array (36 m to 70 m water depths). The other two groups, comprised of, respectively, the PA2, PA1 and Chayvo sites and the AD1, PA1 and Chayvo sites, are similarly representative of the northern and southern ends, respectively, of the more inshore monitoring regime with water depths of 26 - 40 m. The derived parameters of Table 1 include propagation speed, s , and direction, θ , defined in terms of positive clockwise rotations from a due-westward reference direction. Separate values of attenuation coefficients, α , corresponding to wave amplitudes satisfying $A(x)/A(x=0) = e^{-\alpha x}$ for displacements, x , in the direction of wave propagation, are also listed. Values of the latter coefficient were derived using amplitude comparisons along the two constituent paths of each group and division by the cosines of their respective angular deviations from the inferred propagation direction (θ). The, roughly, 0.5 hour uncertainties in estimated signal arrival times limited the accuracies of the obtained wave directionalities and speeds to approximately +/- 3° to 4° and +/- 10 %, respectively.

These results suggest that, as anticipated, the wave disturbances propagated onto the central East Sakhalin shelf with almost due westward directionalities. There is also evidence for a small but consistent rightward (northward) turning of the propagating disturbance in the shallower, more western and northern areas associated with the AD1 and PA2 vertex groups. The attenuation coefficients for the outermost, PA3, vertex region are lower by a factor of 2.7 than expectations based upon Wadhams et al. (1988) measurements and identified concentration and thickness dependences. This discrepancy is explicable if larger floe sizes (80-90 m versus 20-30 m) can be assumed to have been prevalent in our study area. Such an assumption is not unreasonable, given the larger average ice thicknesses noted at PA3 and the site’s greater distance from the pack ice edge relative to the Wadhams et al. (1988) measurement locale. The higher values of α deduced for the PA1 and AD1 vertex areas are (ignoring the discrepancy between the 2 alternative AD1 estimates) consistent with expectations from the observed westward (shoreward) and northward thickening of the pack ice. The general magnitudes of the internally consistent PA2 vertex data are comparable to those obtained by Wadhams et al. (1988) for thicker East Greenland and Greenland Sea ice.

Table 1. Propagation and amplitude attenuation parameters for waves-in-ice as derived from non-parallel measurement paths for each selected group vertex.

Group Vertex	Other Member Sites	s (m/s)	q (°)	a (10^{-5} m^{-1}) by member pair
PA3	PA2, AD1	1.85	-7.4	1.30 (PA3-PA2), 1.49 (PA3-AD1)
PA2	PA1, Chayvo	0.72	+4.0	5.36 (PA2-PA1), 5.22 (PA2-Chayvo)
AD-1	PA1, Chayvo	1.17	+1.6	1.52 (AD1-Chayvo), 3.08 (AD1-PA1)

The most anomalous features of the results in Table 1 are the consistently low propagation speeds which decrease with westward displacement in the directions of positive concentration and thickness gradients. The estimated values are approximately one order of magnitude lower than theoretically derived waves-in-ice group speeds (Wadhams, 1986). These low speeds and the accompanying large wave amplitudes are strongly reminiscent of 1986 shipboard observations in the Weddell Sea as reported in Liu and Mollo-Christensen (1988). In that instance, waves, also of approximately 1 m amplitudes, were observed in ice of similar thickness and high concentrations but at somewhat lower frequencies (18 s wave periods) and even further, 560 km, from the ice edge. The spatial wavelengths associated with these waves were significantly shorter than open ocean gravity waves of the same temporal frequency but gradually lengthened during the break-up of the ice cover which accompanied the event. The Liu and Mollo-Christensen (1988) interpretation of these observations was that internal ice stress altered the coupled ice-ocean wave dispersion relationship to produce very low wave group velocities which produced locally high concentrations of wave energy which broke up the ice cover and altered its subsequent wave propagation properties. Nevertheless, even without accounting for more fundamental objections (Squire, 1995) to the explicit treatment of the ice cover as a uniform medium, the Liu and Mollo-Christensen mechanism is unlikely to have been factor in the Sea of Okhotsk waves-in-ice event. Thus, although the ice in question was exposed to very large stresses by shoreward wind forcing and westward drift, this exposure occurred prior to the, roughly, 1800, March 20, first appearance of wave activity. Such activity was subsequent to the notable east to north wind rotation and the accompanying rapid, latitude-dependent southward ice drift which produced the ice divergences identified above as essential precursors of significant wave amplitudes. It is extremely unlikely that high stress levels, necessarily aligned, according to the Liu and Mollo-Christensen mechanism, with the westward anomalous wave propagation direction, could have been sustained over the, roughly 24 hour duration of high wave activity in the diverging, rapidly southward-drifting pack ice.

Instead, a reasonably consistent explanation or, at least, description of event details can be constructed in terms of a rapid transition in ice cover wave transmissivity initiated by ice divergence. It is not yet clear, on the basis of data from our single event, whether such a transition always accompanies high divergence periods or whether the magnitudes of the changes observed were a consequence of the divergence period following so closely on the heels of a major compression/deformation interval. The latter circumstances left little time refreezing and consolidation of the deformed ice pack, possibly lowering its resistance to dispersal under the subsequent divergent forcing. A basic assumption in this alternative approach is that the slow observed progress of wave activity through the ice pack (i.e. the very low propagation speeds listed in Table 1) represents the spatial advance of a transition from low to high ice wave transmissivity driven by the combined presence of divergence and the incident wave field. The actual phase and group velocities of waves propagating in the offshore, high transmissivity portion of the ice cover need not differ significantly from expectations in terms of conventional coupled propagation models (Wadhams, 1986). In its simplest form, this interpretation postulates a westward- and northward-propagating transition from very high local wave attenuation coefficients to values corresponding to the values listed in Table 1 for the PA2 and PA3 vertex areas, respectively.

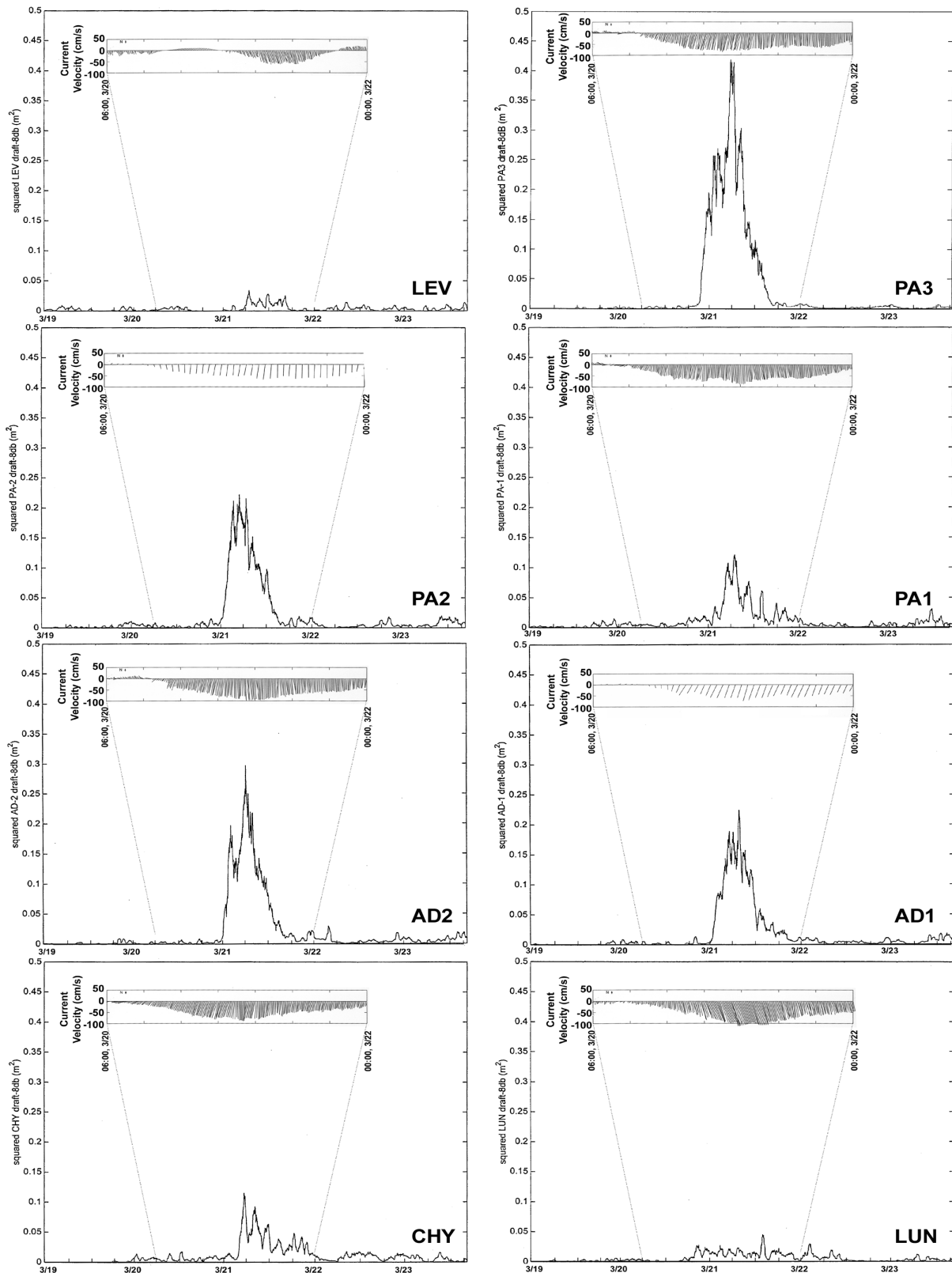


Figure 5. Filtered wave intensity-8dB plotted as a function of time in the period; 0000, March 19 – 1600, March 23 for each of the JIP sites. Stick plot representations of currents are included for each site as indicated for the period, 0600, March 20 through 0000, March 22.

In this view, the negligible wave-in ice amplitudes observed at Levenshterna are a consequence of the local absence of such a transition due to the negligible amounts of divergence observed in the northern portion of the study area immediately subsequent to the massive westward ice movements. Likewise, oscillatory wave amplitudes at the westernmost Chayvo and PA1 sites can be attributed to southward drift of alternating bands of higher and lower attenuation ice across the incident wave paths. Detailed comparisons with the time evolution of the regional wind field and the SSM/I-derived ice pack configurations confirm that this simple model is consistent with the observed time dependences of the wave amplitudes. Quantitative relationships remain to be derived to account for the mechanisms whereby divergence rapidly transforms deformed, compacted ice into a medium of markedly higher wave transmissivity.

CONCLUSIONS

Given an appropriate combination of external wave generation and mechanical ice pack modification processes, very large (mean amplitudes $> 1\text{m}$) waves can be observed for prolonged, 12-18 hr, periods in 1-2 m thick ice several hundred km inside a marginal ice zone. In the case at hand, an intense ice convergence-divergence sequence allowed penetrations of such activity into nominally well-sheltered shelf areas of the Sea of Okhotsk. Nevertheless, limited quantitative understandings (Meylan et al., 1997) of wave responses of realistic ice covers to large-scale strain and forcing leave considerable uncertainties as to the frequencies and extreme amplitudes which could be associated with similar phenomena in a given marginal zone.

REFERENCES

- Liu, A.K. and E. Mollo-Christensen, 1988. Wave propagation in a solid ice pack. *J. Phys. Oceanogr.* **18**, pp. 1702-1712.
- Meylan, M.H., V.A. Squire and C. Fox, 1997. Toward realism in modeling ocean wave behavior in marginal ice zones. *J. Geophys. Res.* **102**, pp. 22981-22991.
- Squire, V.A., 1995. Geophysical and oceanographic information in the marginal ice zone from ocean wave measurements. *J. Geophys. Res.* **100**, pp. 997-998.
- Wadhams, P. 1986. The seasonal ice zone. in *The Geophysics of Sea Ice* (N. Untersteiner, ed.), Plenum Press, New York and London, pp. 825-991.
- Wadhams, P., V.A. Squire and D.J. Goodman, 1988. The attenuation rates of ocean waves in the marginal ice zone. *J. Geophys. Res.* **93**, pp. 6799-6818.